CHARACTERIZATION OF HIGH PERFORMACE SHORT CARBON FIBER/ EPOXY SYSTEMS: EFFECT OF FIBER LENGTH

Paolo Feraboli[1]
Aeronautics and Astronautics
University of Washington
Seattle, WA

Michael J. Graves
Advance Structures Technology
Boeing Phantom Works
Seattle, WA

Patrick B. Stickler
787 Technology Integration
Boeing Commercial Airplanes
Seattle, WA

Abstract

This paper seeks to quantify the influence of fiber length on the mechanical properties of discontinuous carbon fiber/ epoxy laminates produced by compression molding. New interest is being generated toward low-cost composite material forms for aerospace applications. The high-volume carbon fiber content, combined with aerospace-qualified epoxy resins, opens up opportunities for more aircraft parts to be made of non-metallic materials. The Boeing 787 Dreamliner uses this material form for the manufacturing of the structural window frames. This material-process combination is ideal for large volume production of three-dimensional parts, allowing for the molding of complex contours, thickness variations, and stiffening ribs. Interesting relationships between fiber length and tensile, compressive, and flexural moduli and strengths are observed.

Introduction

Airframe components fabricated from composite materials have traditionally been a costly alternative to aluminum construction. The primary challenge that the aerospace industry had to face leading up to the 787 was to fully obtain the performance benefits of composite materials while dramatically lowering production costs [1,2]. Recent composite technology research and development efforts have focused on new low-cost material product forms, and automated processes that can markedly increase production efficiencies. For example, efficient automated tape laying techniques have been developed in the last five years for manufacturing the integrally stiffened fuselage sections [1]. Other examples of non-autoclave material forms used in that effort were the circumferential frames, manufactured via resin infusion of braided preforms, a technique that enables the manufacturing of high-volume components at rapid rates and low recurring costs [1].

[1] Corresponding author: Department of Aeronautics and Astronautics, University of Washington, Box 352400 Seattle, WA 98195-2400 USA

In components exhibiting fully three-dimensional geometry, where the state of stress is not easily predicted or is known to be approximately equal in all directions, such as structural fittings, significant cost and weight savings can be achieved with the use of discontinuous fiber molding compounds for medium or large volume production. For such applications, unidirectional composite prepreg can't be employed in an economically advantageous way due to its labor-intensive nature and poor ability to be draped over complex contours. Machined aluminum parts can be economically viable to produce, but are not compatible with carbon-fiber intensive airframes and lead to heavier designs. With rare exceptions, titanium castings can't be used competitively because of he high casting factors, while titanium forgings rarely offer an economic advantage due to material waste and machining costs.

The interest of the aerospace community for short fiber composites dates back to the 1960s and the pioneering work of Halpin, Pagano, and Kardos [3-5]. Furthermore, Sheet Molding Compounds (SMC) secondary and tertiary airframe structures for non-interior applications have been in service for several years. These compression molding systems typically feature one-inch (25.4 mm) long glass fibers and less than 40% epoxy resin by volume. Although their lower mechanical properties has traditionally limited their range of application, relatively large structures such as engine strut fairings have been in service for several years. In order to become attractive for more significant secondary as well as primary structures, higher performance fiber, resins and manufacturing methods are required. This study investigates the behavior of a high-performance SMC system that uses discontinuous carbon fiber/ epoxy obtained from high-grade prepreg. Commercial applications for this type of material form already exist, although using different resin systems and fiber types and lengths, under various manufacturers and denominations, for example Quantum Lytex 4149, YLA MS-1A, and Hexcel HexMC. Hexcel HexMC is used on the Boeing 787 Dreamliner for manufacturing the first composite structural window frame for a commercial airliner application [1]. The compression-molded composite window frames allow for a 50% weight saving and superior damage tolerance compared to a traditional aluminum frame.

Materials fabrication and test setup

Material Fabrication

Discontinuous carbon/ epoxy panels are manufactured in the laboratory starting from the unidirectional prepreg, which has a resin content of 34%.

In order to obtain a 10 in. x 10 in. (254 mm x 254 mm) 8-ply laminate, 800 in^2 (0.52 m^2) of prepreg are cut from the roll (eight plies of 100 in^2), or 0.065 m^2). Only one ply at a time is cut while the others are stored in the freezer to avoid tacking of the resin. Each ply is clamped down (Figure 1) at one end with an ad hoc fixture, and cut into 10 in. (254 mm) long and 0.3 in. (7.6 mm) wide strips. While clamped, each strip is cut into chips (or ribbons) of desired length. The fiber lengths investigated are 0.5, 1.0, 1.5, 2.0, and 3.0 inches (12.7, 25.4, 38.1, 50.8, 76.2 mm). After removal of the backing tape, the chips are then set into the freezer to maintain low viscosity and prevent premature curing.

In order to obtain an in-plane random distribution, the chips are scattered into a tray and shuffled until visual randomization is achieved (Figure 2). The random stack of chips is then press molded in an aluminum tool for 1 hour at 270° F (132° C) under 800 psi (5.5 MPa) of pressure. The nominal laminate thickness is 0.08 in (2.0 mm).

As the cured plate is removed from the tool, it exhibits several areas of evident defects around the edges, which include both resin-rich and resin-starved spots and voids (Figure 3). Micrographic pictures of center and outermost sections are shown in Figures 4 and 5 respectively. Preliminary results of image analysis appear to show around 0.48% voids for the center section, and about 1.5% for the edges, which are rejected. Removing the peripheral portions of the plate by often more than 1 inch in every direction greatly reduces the effective panel area (Figure 6) from which test specimens (Figure 7) can be extracted. As chip length increases, fabrication becomes more difficult due to the poorer mold-coverage ability of the longer chips and the, hence the tendency to distribute in a less uniform manner. Therefore the effective area suitable for mechanical characterization progressively diminishes as the chip length increases from 0.5 to 3 inches (12.7 to 76.2 mm). The large property variation typical of these materials would suggest testing several specimens per configuration in order to build a statistically significant database. However, the complexity of manufacturing of these panels is such that for this preliminary investigation only 7 specimens per test type and fiber length were tested. All values reported in the results section are the average over these specimens.

For comparison purposes, continuous fiber panels are molded using the same pressure and temperature profiles. Unidirectional and quasi-isotropic [0/90/+45/-45] lay-ups are chosen for the purpose of validating unidirectional lamina values, and to obtain a reference value, or upper bound, for the quasi-isotropic properties to be expected from the discontinuous panels. In flexure, a quasi-isotropic $[90_2/+45_2/-45_2/0_2]_s$ lay-up is also tested to obtain a lower bound for this kind of laminate. Lastly, in order to substantiate the in-plane isotropy of the molded panels, hence the accuracy of the randomization process, three tension specimens for each of the 0, 45, 90 directions are also machined.

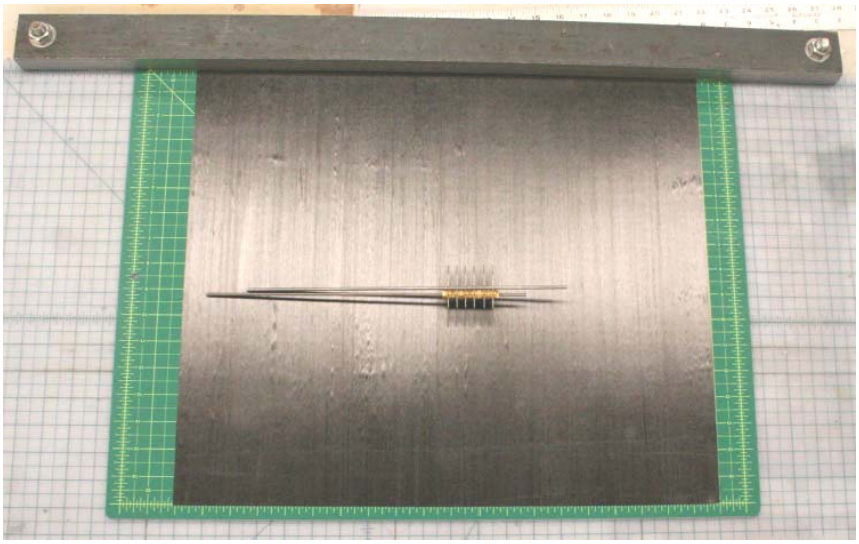

Figure 1. Cutting tool and clamping fixture used to perform the longitudinal slitting of prepreg.

Figure 2. Random distribution of prepreg chips before curing.

Figure 3. Random distribution of prepreg chips after curing, forming a raw laminate.

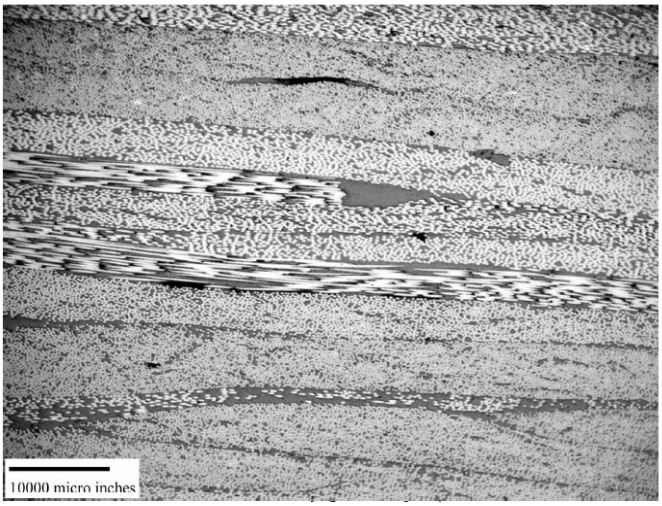

Figure 4. Micrographic picture showing void content in the central (good quality) portion of the “laminate”.

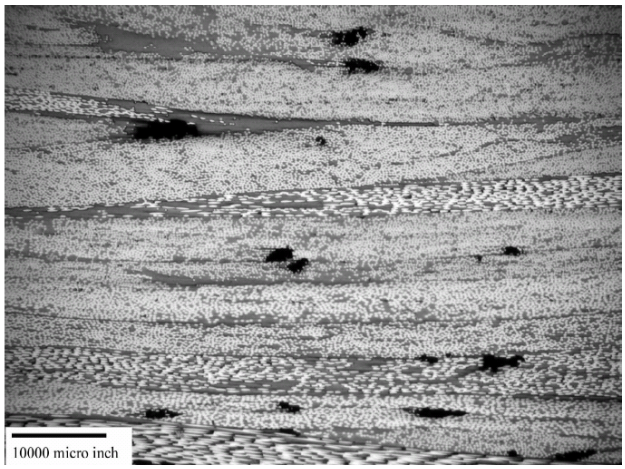

Figure 5. Micrographic pictures showing void content in the peripheral (poor quality) portions of the “laminate”.

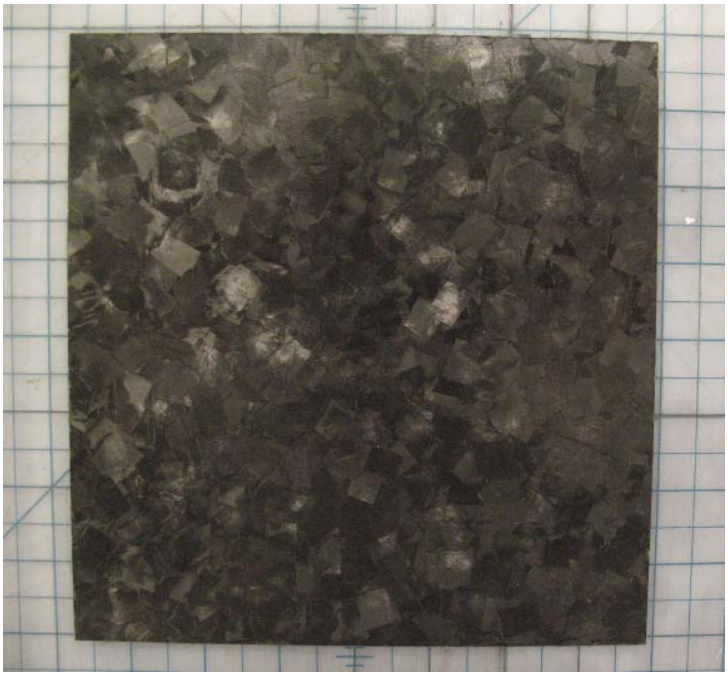

Figure 6. The laminate after cure is machined to remove the poor quality edges, and the usable area is reduced.

Figure 7. Typical tensile test specimens with glass fiber/ epoxy tabs.

Test setup

Tensile, compressive and flexure tests are performed to investigate the influence of chip length. All specimens are loaded to failure at a rate of 0.05 in/min. (1.3 mm/min) in a 2-grip hydraulic tension/ compression test frame. Tensile tests are performed in compliance with standard ASTM D3039 [6], using a 1 in. wide (25.4 mm) and approximately 8 in. (203 mm) long straight specimen. Longer specimens would have been desirable but it was not possible to obtain high quality areas from the molded panels that were longer than 10 inches. Glass/ epoxy tabs are bonded to the specimen

using 3M Scotchweld film adhesive. Compressive tests are performed using the modified ASTM D695 standard [7]. Specimens 0.5 in. wide (12.7 mm) and 3.2 in. (81.3 mm) long are cut from each plate. The specimens are fitted with glass/ epoxy tabs as prescribed by the standard. Flexure tests are performed in compliance with standard ASTM D790 [8]. All specimens are loaded to failure in three-point bending using a span of 2.0 inches (50.8 mm), which gives a span to thickness ratio of 33, is selected to accommodate all specimens due to minor variations in thickness. Specimen width is constant at 0.5 in (12.7 mm). For tensile and compressive tests, modulus is measured with an extensometer, while for flexure tests the modulus is calculated according to ASTM directions.

For the present study, all strength data reported in the following sections refers to ultimate strength, calculated as the strength corresponding to ultimate load. Ultimate load is determined as the highest value of load reached in the load-displacement curve before a large drop, usually to values of half the previous ones.

Results

Tension

Typical tensile load-displacement curves are shown in figure 8, which shows how there appear to be three kinds of behaviors following the initial linear range. The first (A) sees the occurrence of one or more small drops in the curve, associated to the onset of failure, followed by catastrophic failure, where the load drop is in the order of ten times the remainder load carrying capability. The type of failure occurring initially has not yet been identified, as it could involve matrix cracking, chip/ matrix disbanding or fiber breakage. In the second family of curves (B), these preliminary failures are not observable and the specimens transitions abruptly from the linear regime to ultimate load and catastrophic failure. The last family (C) sees the onset of ultimate load followed by a step-type ramp of progressively decreasing load bearing capability, in a fashion much less catastrophic then the former two.

In rare occasions the specimens have fractures into two pieces, while in the vast majority of cases they maintain integrity after reaching ultimate load (figure 9). Failed specimens feature several “delaminations” through the thickness, or separation of multiple chip in a single stack. The nature of failure modes and the cause that generate these different behaviors have not yet been identified.

Micrographic pictures of Figures 10 a-c show progressively closer views of a failed specimen. The fracture surfaces are distinctly divided in two, and appear to have slid relative to each other. Multiple surfaces are visible through the specimen thickness, which indicate that fracture changes path longitudinally and transversely wherever it may be easier. It is interesting to observe that not a single chip, but rather a wedge consisting of several chips tends to pullout from the other half of the specimen. The random orientation of the chips and of the individual fibers is clearly visible, as well as a large central resin-rich area. Figures 11 a-c shows a similar micrographic image of another specimen, which highlights other interesting observations. There are two distinct failure locations, one to the left of Figure 11 a, which resembles the one discussed before, and the other to the far right, which is the one shown in greater detail in Figures 11 b and c. The latter one is of interest as it clearly highlights a combination of two failure modes between and within individual chips: cracking, or separation along a plane perpendicular to the chip axis, and “delamination”, or separation along a plane parallel to the chip’s length. Brittle fracture seems to start toward the surface, as tensile matrix failure,

progress through a few chips, then eventually transform into delamination of one long chip from the remainder “laminate”. Counter-intuitively, the path of least resistance does not necessarily follow a resin-rich are (as shown in Figure 11 c), a void, or a chip edge within the polished plane, since the neighboring chips (not visible) may offer different degrees of crack arrest.

Results for the ultimate strength and elastic modulus are plotted as a function of chip length in Figures 12 and 13 respectively. Error bars represent standard deviation for the seven specimens tested per configuration.

For reference, the average value of the continuous quasi-isotropic laminate is also traced on the plot, without its associated CoV band. Ultimate tensile strength is shown to increase monotonically with chip length, but remains noticeably lower than the continuous QI value. On the other hand, modulus appears to increase negligibly in the range of chip lengths investigated, and overall it is equal or only slightly lower than the QI reference. According to well-established literature [4-6], the critical aspect ratio for discontinuous fiber systems is given by l/d (fiber length/ fiber diameter) and it usually is around 200. In the case of chip (or ribbon) reinforcement, the ratio of l/t (chip length/ chip thickness) rather than l/w (chip length/ chip width) should be taken. For the investigation at hand, l/t ranges between 72 and 430, therefore it seems to suggest that the critical aspect ratio lies somewhere in between, possibly around 1.5 inches. However, the variation is so minimal at the smaller lengths that it appears shorter reinforcements could be used without severe penalties from an elastic modulus standpoint.

Results from tension tests of the specimens machined at 0, 90 and 45 degrees from the assumed longitudinal direction, which corresponds to the one perpendicular to the body of the operator performing the process, are also shown in table 1. It can be seen that there is a 20% bias in the average ultimate strength between the 0 and the 90 degree values, while the 45 degree value is well in line with the 0 value. It should be kept in mind that only three off-axis specimens were tested to obtain these average strengths, and that given the high variation observed in these panels such observation is not conclusive. Yet, it seems to suggest that there is an acceptable amount of repeatability in the process, and that the molded panels behave as in-plane pseudo-isotropic fashion.

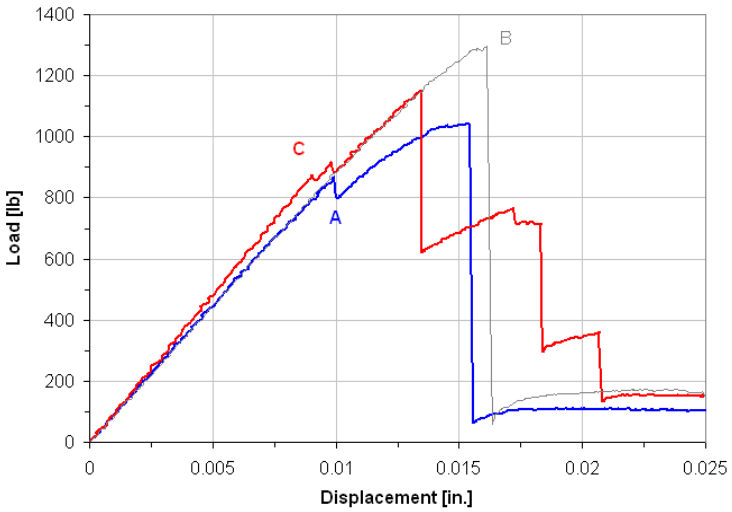

Figure 8. Typical tensile load-deflection curves observed show three different behaviors

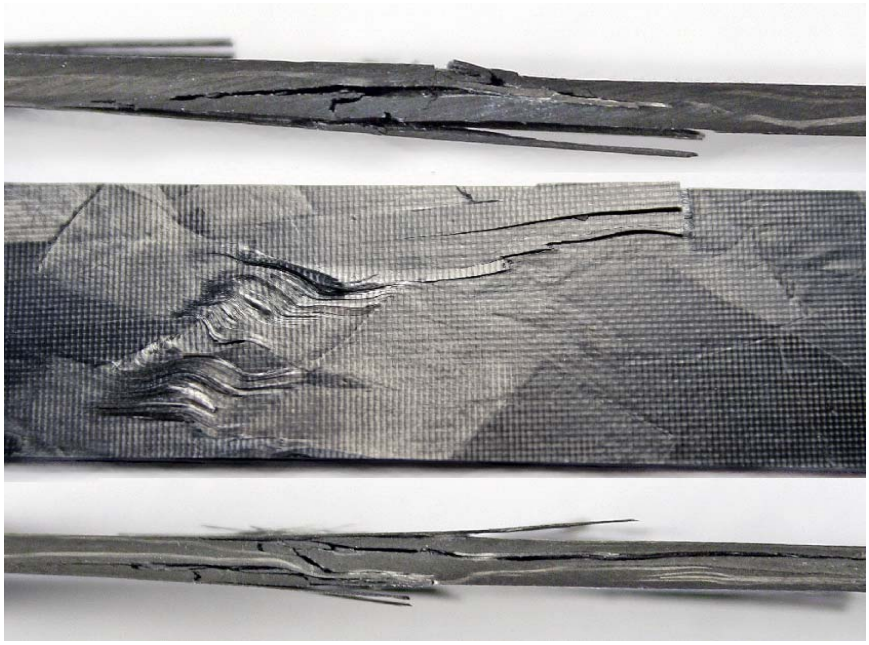

Figure 9. Typical morphology of tension failed specimen, top and side views.

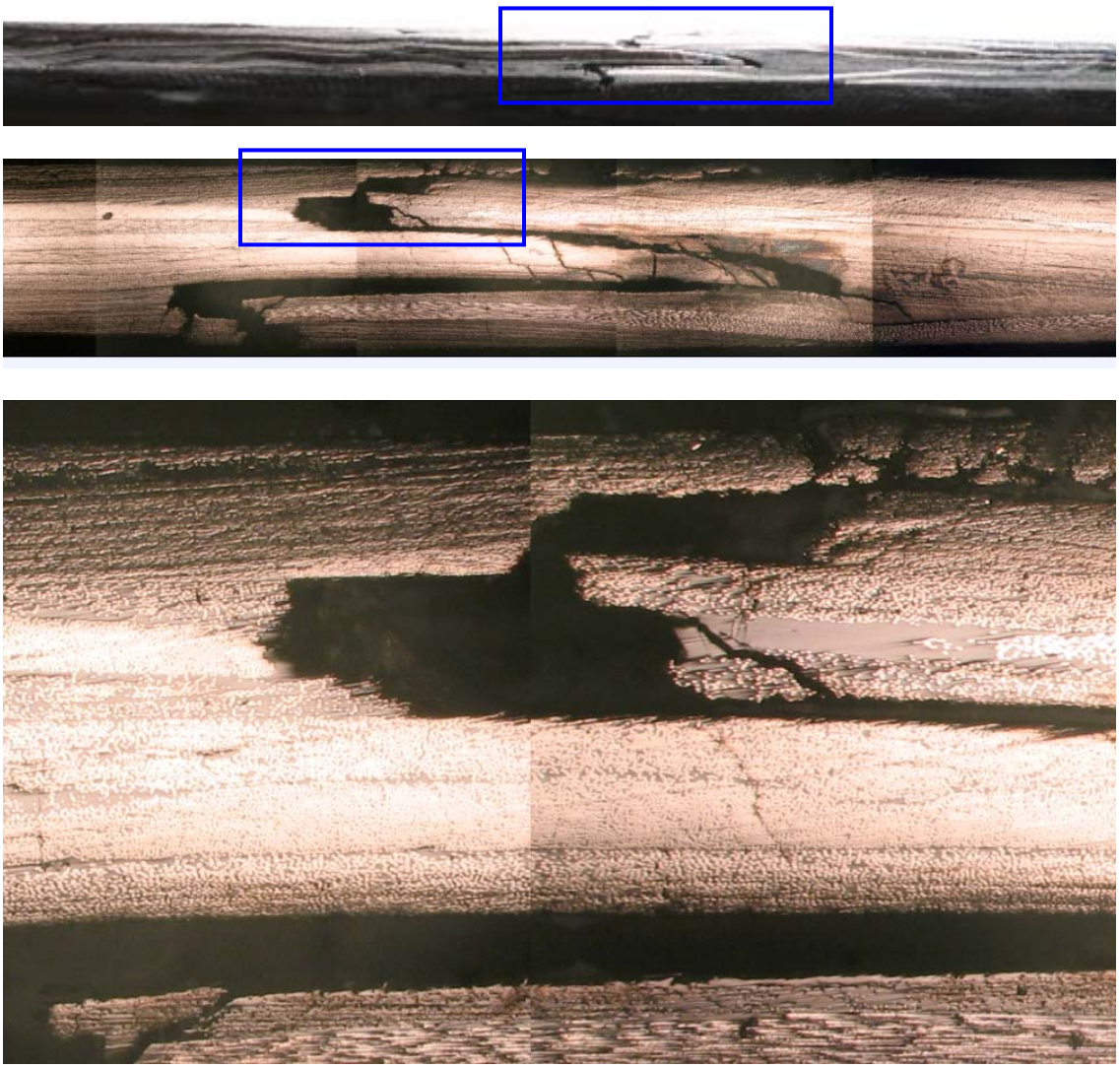

Figure 10 a-c. Sequence of micrographic pictures at increasing magnification of typical tension failed specimen, primary failure.

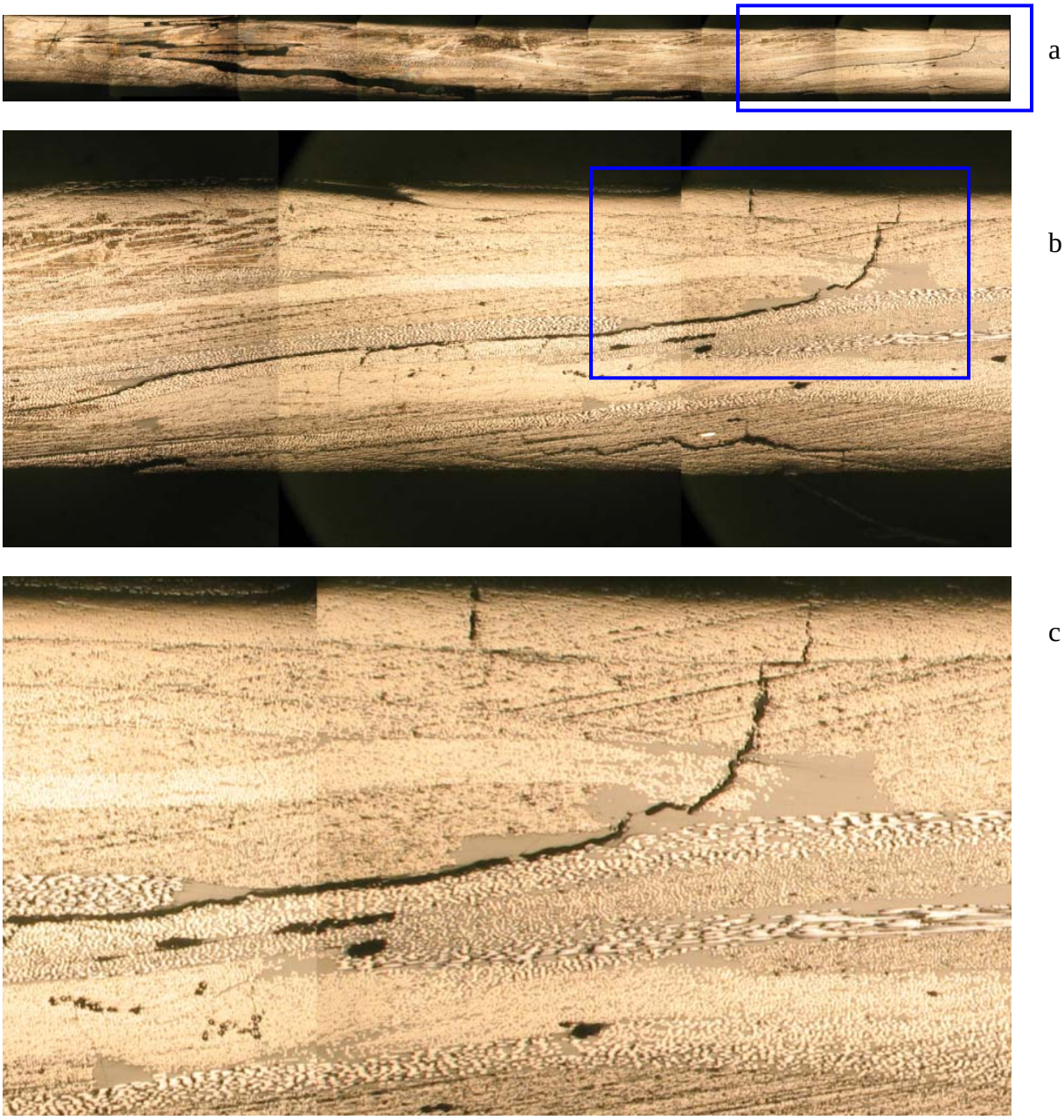

Figure 11 a-c. Sequence of micrographic pictures at increasing magnification of typical tension failed specimen, secondary failure.

Table 1. Tensile results for panel used to verify degree of in-plane isotropy.

Configuration	Tensile Strength [ksi]	CoV [%]	Tensile Modulus [Msi]	CoV [%]	No. tests
0	36.7	3	6.5	13	3
45	38.9	24	6.7	21	3
90	55.6	17	7.2	23	3

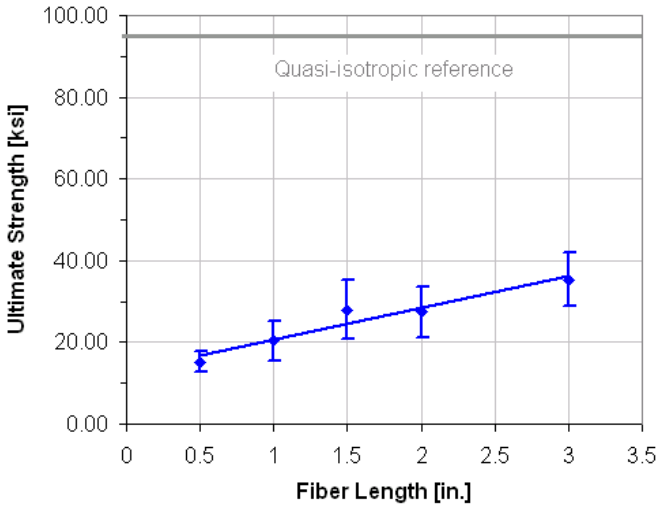

Figure 12. Average tensile ultimate strength plotted as function of chip length, with continuous fiber quasi-isotropic as reference.

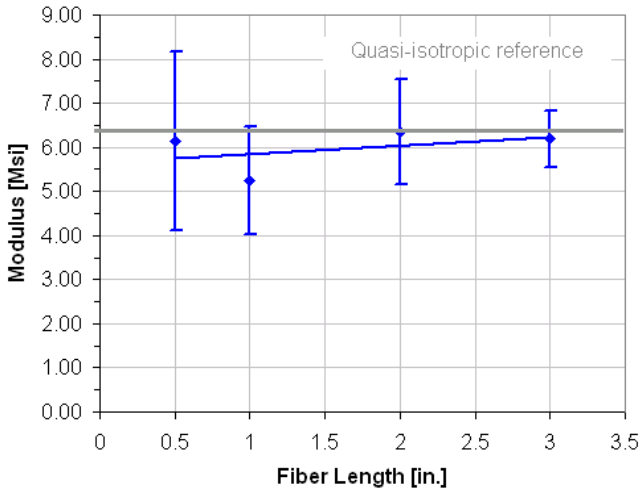

Figure 13. Average tensile modulus plotted as function of chip length, with continuous fiber quasi-isotropic as reference.

Compression

Typical compressive load-displacement curves are shown in Figure 14. It can be seen that these curves show the same three families of behavior corresponding to a series of smaller failure prior to ultimate failure (A), sudden drop from ultimate load (B), and lastly a less abrupt failure through progressive smaller drops from ultimate load (C). All specimens show good compression failure by fiber breakage, and "sublaminate" separation. This separation is visible in Figure 15, where a wedge comprising several chips (similar to the tensile case) tends to slide into the other portion of the specimen.

Ultimate strength and modulus results are also plotted against chip length in figures 16 and 17 respectively. Similar trends to the tension case can be see in both plots, however the ultimate strength in compression is closer to the QI value than in tension. Also, the modulus seems to increase more markedly between the shorter and longer reinforcements tested. In general, results confirm that the continuous QI and discontinuous prepreg perform equally well from a stiffness perspective, but strength is noticeably lower for the discontinuous fiber system.

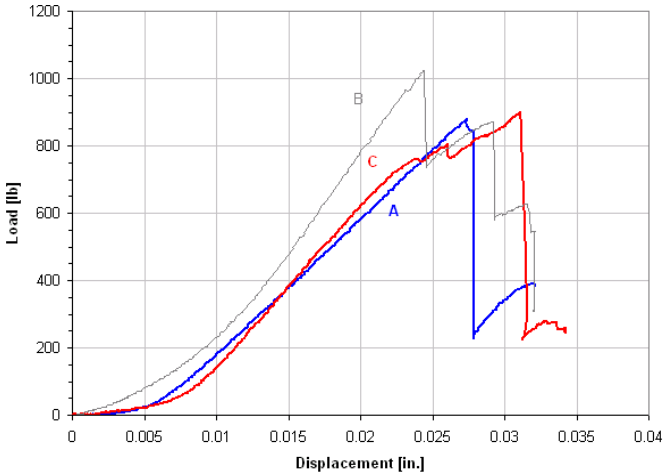

Figure 14. Typical compressive load-deflection curves observed show three different behaviors

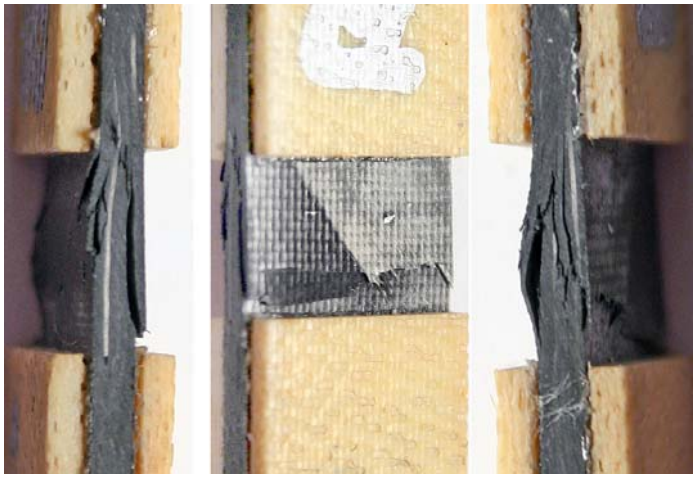

Figure 15. Typical morphology of tension failed specimen, top and side views.

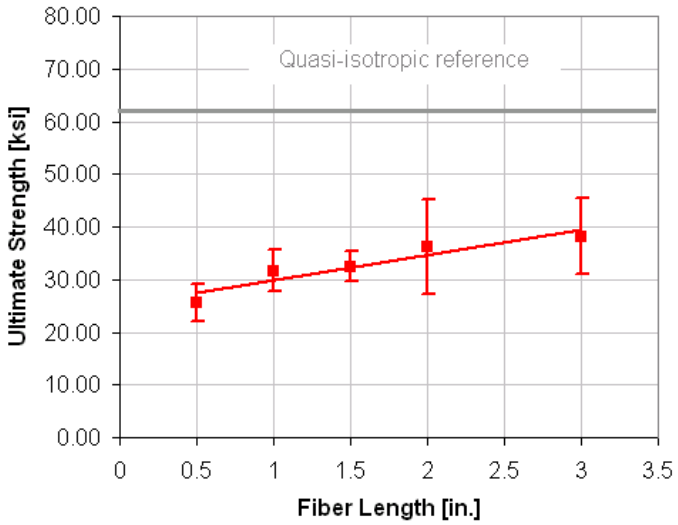

Figure 16. Average compressive ultimate strength plotted as function of chip length, with continuous fiber quasi-isotropic as reference.

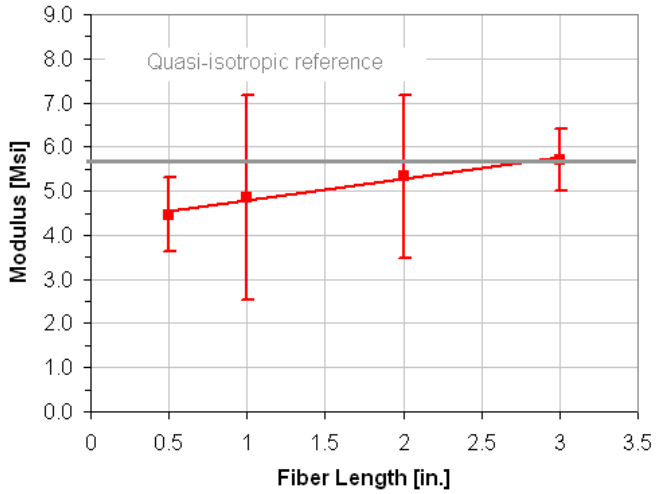

Figure 17. Average compressive modulus plotted as function of chip length, with continuous fiber quasi-isotropic as reference.

Flexure

Typical load-displacement curves for flexure test are shown in figure 18. For the shorter chip lengths, the curves tend to exhibit a less linear behavior than for the longer chips. Specimens fail by tension on the bottom surface, however in some specimens it does not occur directly below the loading roller where the bending moment is maximum (as shown in Figure 19). This phenomenon, not seen in continuous fiber laminates, can be explained by the heterogeneous nature of this material form.

Ultimate strength and modulus results as function of chip length are shown in Figures 20 and 21. The effects of fiber length appear to markedly influence strength

values, while modulus appears to be less affected. Furthermore, it appears that flexure modulus for the discontinuous fibers may even exceed that of the quasi-isotropic benchmark. However, modulus is calculated using ASTM guidelines, and not measured directly as in the tension and compression cases.

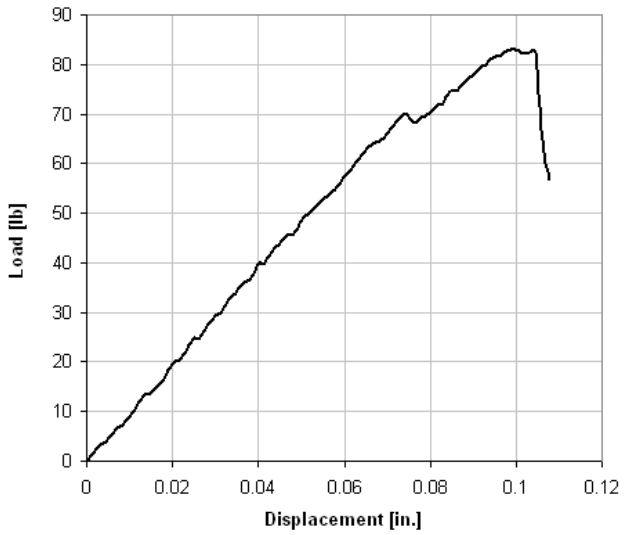

Figure 18. Typical flexural load-deflection curve.

Figure 19. Flexure specimen failing in tension directly below the loading roller.

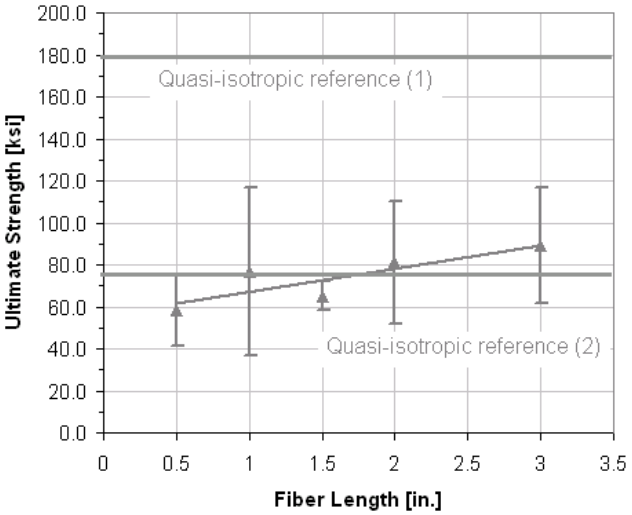

Figure 20. Average flexure ultimate strength plotted as function of chip length, with continuous fiber quasi-isotropic as reference.

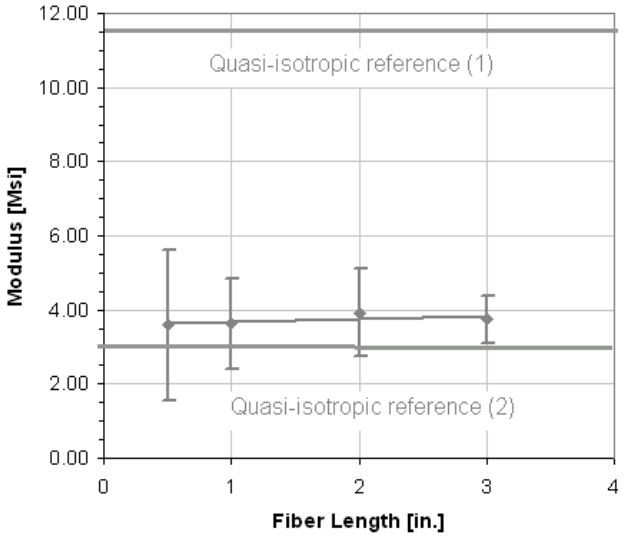

Figure 21. Average flexure modulus plotted as function of chip length, with continuous fiber quasi-isotropic as reference.

Discussion and future work

The trends observed in Figures 12, 16, 20 for tension, compression and flexure strengths respectively are summarized in Figure 22. It is evident that average strength increases monotonically as a function of chip length. The longest chip strength exhibits strengths between 1.4 and 2 times larger than the shortest chip length, according to the load type. From the plot is also clear that flexure strength benefits from longer chip length than tension and compression, which can be explained by the greater “bridging effect” possible in bending of the chip wedge. Flexural strength is consistently the highest, followed by compressive, and then tensile strengths. This behavior differs from

continuous fiber laminates, such as the QI tested in this study, where compressive strength is always lowest, and tensile and flexural strengths are usually closer together.

In a similar fashion to the strength plot, Figure 23 summarizes the trends observed in figures 13, 17, 21 for tension, compression and flexure moduli respectively. Although modulus increases monotonically with respect to fiber length, the situation is somewhat less dramatic than for strength. The average modulus for the longest chip is only 1 to 1.2 higher than the shortest chip modulus, also depending on the loading scenario.

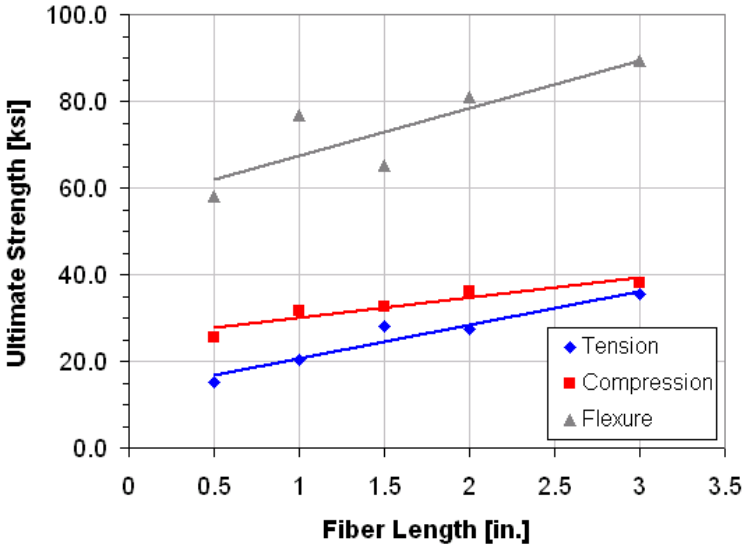

Figure 22. Tensile, compressive and flexural ultimate strengths as function of chip length.

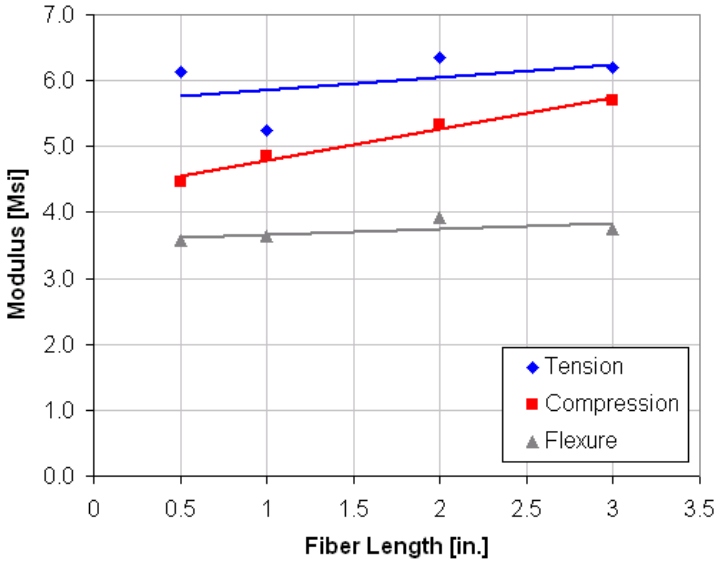

Figure 23. Tensile, compressive and flexural moduli as function of chip length.

With regards to the high variation observed in this study, it should be considered that the manufacturing process used has not been industrialized, and that existing or future commercial systems will inevitably show reduced variation in the mechanical properties, thanks to a more accurate randomization process and better curing methods. Automated chip randomization and assembly will lead to better mold coverage and reduced void content, as well as less possibilities for contamination during the lengthy process of slitting and chipping. The use of more suitable resin systems, with ad hoc developed cure temperature, pressure and time, will also generate more flow in the matrix and thus lead to improved mold coverage and reduced void content.

For the chip geometries investigated, results seem to suggest that using chip l/t to predict the critical aspect ratio may not be suitable, as neither modulus nor strength appear to have reached asymptotic values. If a “chip critical aspect ratio” can be determined, it may be possible to replace the individual fiber aspect ratio and extend the laminate analogy by Halpin et al. [4,5] to chip (or ribbon) reinforced systems.

Increasing strength for increasing fiber length is consistent with traditional observations by Halpin et al., but is in contrasts with recent observations on P4-type systems [9], which use short carbon fiber preforms for liquid resin injection. However, it is likely that the trends of decreasing strength observed there for increasing filament size may be associated with inconsistencies in the manufacturing process, which will change once the process is controlled.

From a mechanical performance standpoint, and limited to the number of specimens and specimen geometries tested, results seem to recommend the use of longer chips. However, longer chips add manufacturing complexities due to the greater possibility for fiber distortion/kinking, resin-rich or resin-starved areas (unwetted zones) as well as greater susceptibility to voids (different from porosity). The tradeoffs between manufacturing characteristics (drapeability, flow, etc.) and mechanical performance need to be further studied, and may lead to the determination of a compromise chip size.

Conclusions

This study investigated the influence of chip (fiber) length on the tensile, compressive and flexural properties of a high-performance SMC system that uses discontinuous carbon fiber/ epoxy obtained from high-grade prepreg. For all load scenarios investigated, the discontinuous systems perform almost equally well as the continuous quasi-isotropic benchmark from a stiffness standpoint, but is noticeably inferior from an ultimate strength standpoint. Further work will be aimed at understanding other characteristics of this material form, such as notched response, and extending the laminate analysis methods used for continuous fiber.

Acknowledgements

The authors wish to acknowledge Dr. Al Miller, Director of Boeing 787 Technology Integration, for supporting this study, and Dr. John Halpin, JCH Consultants, for providing guidance in the project. UW AA Graduate students Elof Peitso, Francesco Deleo and Tyler Cleveland deserve the authors’ recognition for performing specimen preparation and testing. This work would not have been possible without the donation of prepreg material by Andrea Dorr (Toray Composites of America).

References

1. Miller, A.G., “The Boeing 787 Dreamliner”, Keynote Address, 48th AIAA/ASME/ASCE/AHS/ASC Structures, Structural Dynamics, and Materials Conference, Waikiki, HI, 2007.
2. Stickler, P.B., “Composite Materials for Commercial Transport – Issues and future research directions”, Proceedings of the ASC, 17th Annual Technical Conference, West Lafayette, IN, 2002.
3. Halpin, J.C., Pagano, N.J., “The Laminate Approx. for Randomly Oriented Short Fiber Composites”, Polymer Engineering and Science, Vol. 3, 1969.
4. J. C. Halpin, J. L. Kardos. Strength of Discontinuous Reinforced Composites. Polymer Engineering and Science. 18, 6, 1978 (p.496).
5. Kardos, J.L., Michno, M.J., Duffy, T.A., “Investigation of High Performance Short Fiber Reinforced Plastics”, Final Report, Naval Air Systems Command, No. N00019-73-C-0358, 1974.
6. ASTM D3039/D3039M-00, “Standard Test Method for Tensile Properties of Polymer Matrix Composite Materials”, Volume 15.03, 2006.
7. ASTM D695-02a, “Standard Test Method for Compressive Properties of Rigid Plastics”, Volume 08.01, 2002.
8. ASTM D790-03, “Standard Test Methods for Flexural Properties of Unreinforced and Reinforced Plastics and Electrical Insulating Materials”, Volume 08.01, 2003.
9. Harper, L.T., Turner, T.A., Warrior, N.A., Rudd, C.D., “Characterization of random carbon fibre composites from a directed fibre preforming process: The effect of fibre length”, Composite Part A xxx (Article in Press). 8/31/2005.